Supplementary Information

for

A five-component nanorotor with speed regulation

Soumen K. Samanta,[a] Jan W. Bats,[b] Michael Schmittel*,[a]

[a] Center for Micro- and Nanochemistry and Engineering, Organische Chemie I, Adolf-Reichwein Strasse, Universität Siegen, D-57068 Siegen, Germany

schmittel@chemie.uni-siegen.de

[b] Institut für Organische Chemie und Chemische Biologie, Johann Wolfgang Goethe-Universitat, Max-von-Laue Strasse 7, D-60438 Frankfurt am Main, Germany

Contents

1. Synthesis

Experimental Section

General. Commercial reagents like **3** were used without further purification. Solvents were dried with appropriate desiccants and distilled prior to use. Thin-layer chromatography was performed using Merck silica gel TLC plates (silica gel 60 F_{254}). Silica gel 60 was used for column chromatography. ^{1}H and ^{13}C NMR spectra were recorded on Bruker Avance (400 MHz) and Varian (600 MHz) spectrometers using a deuterated solvent as the lock and residual protiated solvent as internal reference. The following abbreviations were utilised to describe NMR peak patterns: s = singlet, d = doublet, t = triplet, dd = doublet of doublets. The following abbreviations were used to describe peak patterns of IR spectra: s = sharp, m = medium, w = weak. The numbering of the carbon skeleton in molecular formulae as shown in the manuscript does not comply with the IUPAC nomenclature rules; it is only used for assignments of NMR signals. Electrospray ionisation (ESI) mass spectra were recorded on a Thermo-Quest LCQ Deca. Melting points were measured on a Büchi SMP-20 and are un-corrected. Infrared spectra were recorded on a Varian 1000 FT-IR instrument. Elemental analysis measurements were made using the EA 3000 CHNS. UV-Vis spectra were recorded on a Varian Cary 100 Bio UV/visible spectrometer. Photoisomerisations were performed in the photoreactor LUMOS 43 from Atlas Photonics.

Complex [Cu(*trans*-3)(4)](PF$_6$)

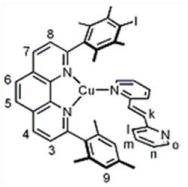

[Cu(*trans*-**3**)(**4**)]$^{+}$

In an NMR tube, 2-(2,3,5,6-tetramethyl-4-iodophenyl)-9-(2,4,6-trimethylphenyl)[1,10]-phenanthroline (**4**), (1.14 mg, 2.05 µmol) and $[Cu(CH_3CN)_4]PF_6$ (0.764 mg, 2.05 µmol) were dissolved in CD_2Cl_2 (0.45 mL). Then, *trans*-**3** (0.374 mg, 2.05 µmol) was added and the mixture stirred for 0.5 h furnishing the desired complex in quantitative yield. Mp: > 300 °C. ^{1}H NMR (400 MHz, CD_2Cl_2) δ = 1.87 (s, 6 H, CH_3), 1.93 (s, 6 H, CH_3), 2.03 (s, 3 H, CH_3), 2.14 (s, 6 H, CH_3), 6.60 (s, 2 H, 9-H), 7.16 (dd, ^{3}J = 8.0 Hz, ^{3}J = 1.6 Hz, 2 H, o-H), 7.22 (s, 2 H, k-H), 7.40 (d, ^{3}J = 8.0 Hz, 2 H, l-H), 7.74 (td, ^{3}J = 8.0 Hz, ^{4}J =1.6 Hz, 2 H, m-H), 7.92 (d, ^{3}J = 8.0 Hz, 1 H, 7-H), 7.96 (d, ^{3}J = 8.0 Hz, 1 H, 4-H), 8.10 (d, ^{3}J = 8.0 Hz, 2 H, n-H), 8.21 (s, 2 H, 5-, 6-H), 8.72 (d, ^{3}J = 8.0 Hz, 1 H, 8-H), 8.73 (d, ^{3}J = 8.0 Hz, 1 H, 3-H) ppm. ^{13}C NMR

(100 MHz, CD_2Cl_2) δ = 2.1 (CH_3 for acetonitrile), 19.8, 20.4, 20.9, 27.4, 113.0, 116.9 (CN of acetonitrile), 123.1, 123.8, 127.1, 127.2, 127.2, 127.4, 128.1, 128.2, 128.4, 132.0, 132.1, 135.5, 137.1, 137.5, 138.2, 139.2, 139.6, 139.7, 140.4, 143.8, 144.1, 149.3, 154.0, 161.3, 161.4 ppm. IR (KBr): ν = 3944 (w), 3691 (w), 3054 (s), 2987 (m), 2686 (w), 2521 (w), 2411 (w), 2306 (m), 1422, 1262 (s), 1156 (w), 896 (m), 753 (s) cm^{-1}. Anal. Calcd. for $C_{43}H_{39}CuF_6IN_4P•H_2O$: C, 53.51; H, 4.28; N, 5.80. Found: 53.86; H, 3.93; N, 6.12.

Irradiation of [Cu(*trans*-3)(4)](PF$_6$)

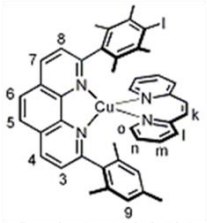

[Cu(*cis*-**3**)(**4**)]$^+$

In an NMR tube, complex [Cu(*trans*-**3**)(**4**)](PF$_6$) was dissolved in dry and degassed DCM (0.45 mL). The sample was irradiated for 2 h at 315 nm. The sample was characterised by ^{1}H NMR. Yield of [Cu(*cis*-**3**)(**4**)](PF$_6$): 70%. ^{1}H NMR (400 MHz, CD_2Cl_2) δ = 1.77 (br s, 12 H, CH_3), 2.07 (s, 3 H, CH_3), 2.17 (s, 6 H, CH_3), 6.08 (s, 1.4 H, k-H, *cis*), 6.58 (s, 2 H, 9-H), 6.93 (dd, ^3J = 8.0 Hz, ^3J = 4.4 Hz, 1.4 H, o-H, *cis*), 7.13 (dd, ^3J = 8.0 Hz, ^3J = 4.4 Hz, 0.6 H, o-H, *trans*), 7.19 (s, 0.6 H, k-H, *trans*), 7.21 (d, ^3J = 8.0 Hz, 1.4 H, l-H, *cis*), 7.37 (d, ^3J = 8.0 Hz, 0.6 H, l-H, *trans*), 7.63 (d, ^3J = 4.4 Hz, 1.4 H, n-H, *cis*), 7.67 (td, ^3J = 8.0 Hz, ^4J =1.6 Hz, 1.4 H, m-H, *cis*), 7.73 (td, ^3J = 8.0 Hz, ^4J =1.6 Hz, 0.6 H, m-H, *trans*), 7.87 (d, ^3J = 8.0 Hz, 1 H, 7-H), 7.92 (d, ^3J = 8.0 Hz, 1 H, 4-H), 8.05 (d, ^3J = 4.4 Hz, 0.6 H, n-H, *trans*), 8.21 (s, 2 H, 5-, 6-H), 8.70 (d, ^3J = 8.0 Hz, 1 H, 8-H), 8.72 (d, ^3J = 8.0 Hz, 1 H, 3-H) ppm. ESI-MS: *m*/*z* (%) 802.4 (100) $[M+H]^+$.

Preparation of ROT-2

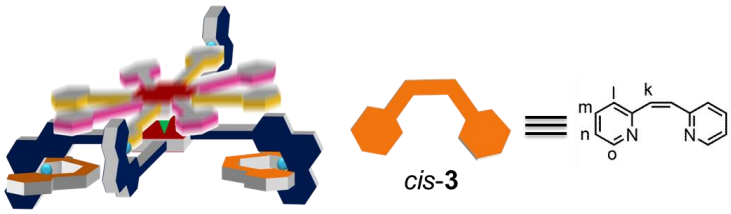

ROT-2 = [(**ROT-1**)(*cis*-**3**)$_2$]

In an NMR tube, **ROT-1** (1.96 mg, 0.445 µmol) and 2.85 equiv. of *trans*-**3** (0.231 mg, 1.27 µmol) were dissolved in dry and deoxygenated DCM (0.45 mL). The solution was irradiated for 2 h at 315 nm to afford **ROT-2** quantitatively based on **ROT-1**. ^{1}H NMR (400 MHz, CD_2Cl_2) δ = −4.56 (s, 6 H, CH_2^{DABCO}), −4.54 (s, 6 H, CH_2^{DABCO}), 1.66 (s, 12 H, CH_3), 1.72 (s, 6 H, CH_3), 1.77 (s, 6 H, CH_3), 1.78 (s, 12 H, CH_3), 2.03 (s, 12 H, CH_3), 2.09 (s, 6 H, CH_3), 2.15 (s, 12 H CH_3), 2.19 (s, 12 H, CH_3), 2.49 (s, 6 H, CH_3), 2.58 (s, 12 H, CH_3), 2.63 (s, 6 H, CH_3), 6.21 (s, 4 H, k-H, *cis*-**3**), 6.50 (d, ^3J = 5.6 Hz, 2 H, d-H), 6.60 (s, 4 H, 9-H, complex with *cis*-**3**), 6.69 (d, ^3J = 5.6 Hz, 1 H, h-H), 6.94 (br s, 1 H, i-H), 6.97 (br s, 4 H, o-H, *cis*-**3**), 7.06 (d, ^3J = 5.6 Hz, 2 H, c-H), 7.10 (s, 4 H, 9-H, HETPYP), 7.24 (d, ^3J = 8.0 Hz, 4 H, l-H, *cis*-**3**), 7.31 (m, 1 H, g-H), 7.34 (s, 2 H, j-H), 7.35 (s, 2 H, j-H), 7.42 (d, ^3J = 4.4 Hz, 4 H, n-H, *cis*-**3**), 7.57 (d, ^3J = 8.0 Hz, 4-H, [10- or 11]-H), 7.64 (td, ^3J = 8.0 Hz, ^4J = 1.6 Hz, 4 H, m-H, *cis*-**3**), 7.79 (d, ^3J = 8.0 Hz, 4-H, [10´ or 11´]-H), 7.86 (d, ^3J = 8.0 Hz, 2 H, 7-H complex with *cis*-**3**), 7.91 (d, ^3J = 8.0 Hz, 2 H, 4-H, complex with *cis*-**3**), 7.95 (d, ^3J = 8.0 Hz, 4 H, [11 or 10]-H), 7.99 (d, ^3J = 8.0 Hz, 4 H, [a, e]-H), 8.01 (d, ^3J = 8.0 Hz, 4 H, [11´ or 10´]-H), 8.03 (d, ^3J = 8.0 Hz, 4 H, 4-, 7-H, HETPYP), 8.20 (s, 4 H, 5-, 6-H, complex with *cis*-**3**), 8.26 (s, 4 H, 5-, 6-H, HETPYP), 8.29 (d, ^3J = 8.0 Hz, 4 H, [b, f]-H), 8.36 (d, ^3J = 4.4 Hz, 4 H, β-H), 8.37 (d, ^3J = 4.4 Hz, 4 H, β-H), 8.56 (d, ^3J = 4.4 Hz, 4 H, β-H), 8.57 (d, ^3J = 4.4 Hz, 4 H, β-H), 8.69 (d, ^3J = 8.0 Hz, 2 H, 8-H, complex with *cis*-**3**), 8.70 (d, ^3J = 8.0 Hz, 2 H, 3-H complex with *cis*-**3**), 8.80 (d, ^3J = 8.0 Hz, 4 H, 3-, 8-H, HETPYP) ppm. ESI-MS: *m*/*z* (%) 1046.2 (100) [(**ROT-1**)(*cis*-**3**)$_2$]$^{4+}$ and 1443.3 (70) [(**ROT-1**)(*cis*-**3**)$_2$](PF$_6$)$^{3+}$.

ROT-2 is present at the PS state aside of 0.85 equiv. of *trans*-**3** as characterised by ^{1}H NMR (Figure S11) and ^{1}H-^{1}H COSY (Figure S12) spectra. ^{1}H NMR (400 MHz, CD_2Cl_2) of *trans*-**3**: δ = 7.17 (dd, ^3J = 8.0 Hz, ^3J = 4.4 Hz, 2 H, o-H, *trans*-**3**), 7.32 (s, 2 H, k-H, *trans*-**3**), 7.48 (brs, 2 H, l-H, *trans*-**3**), 7.71 (td, ^3J = 8.0 Hz, ^4J = 1.6 Hz, 2 H, m-H, *trans*-**3**), 7.78 (brs, 2 H, n-H, *trans*-**3**) ppm.

2. NMR Spectra

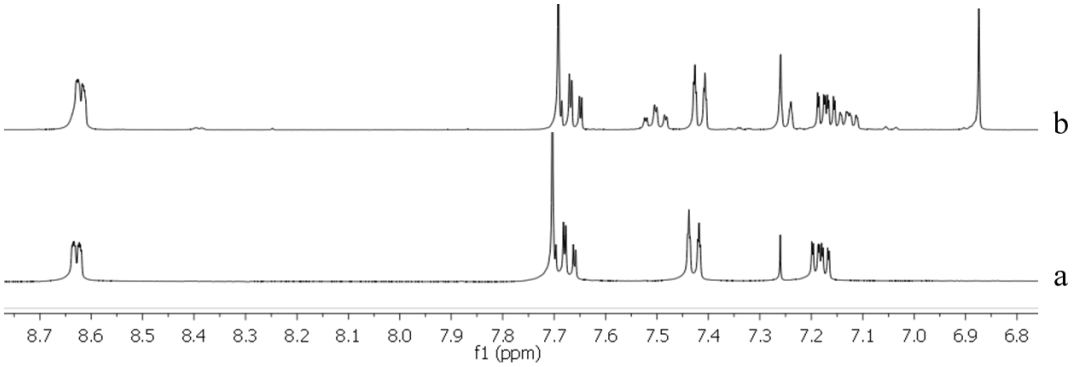

Figure S1. Partial ^{1}H spectra (400 MHz, $CDCl_3$, 298 K) of (a) *trans*-**3**, and (b) of **3** after irradiation for 2 h at 315 nm (*trans*:*cis* = 62:38) in DCM.

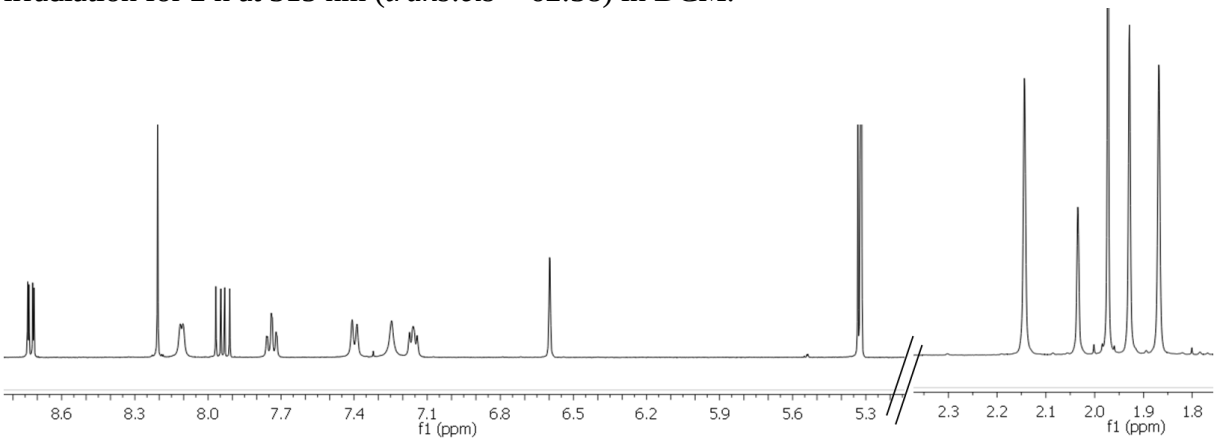

Figure S2. ^{1}H NMR spectrum of [Cu(*trans*-**3**)(**4**)]PF_6 (400 MHz, CD_2Cl_2, 298 K).

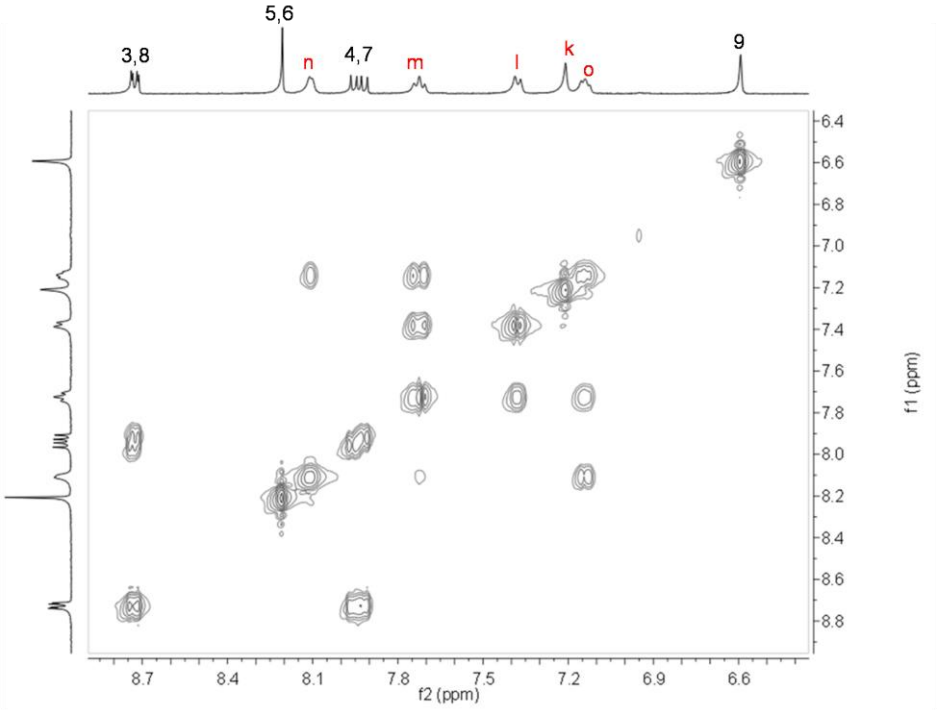

Figure S3. ^{1}H-^{1}H COSY spectrum of [Cu(*trans*-**3**)(**4**)]PF_6 (400 MHz, CD_2Cl_2, 298 K). Protons for *trans*-**3** are shown in red.

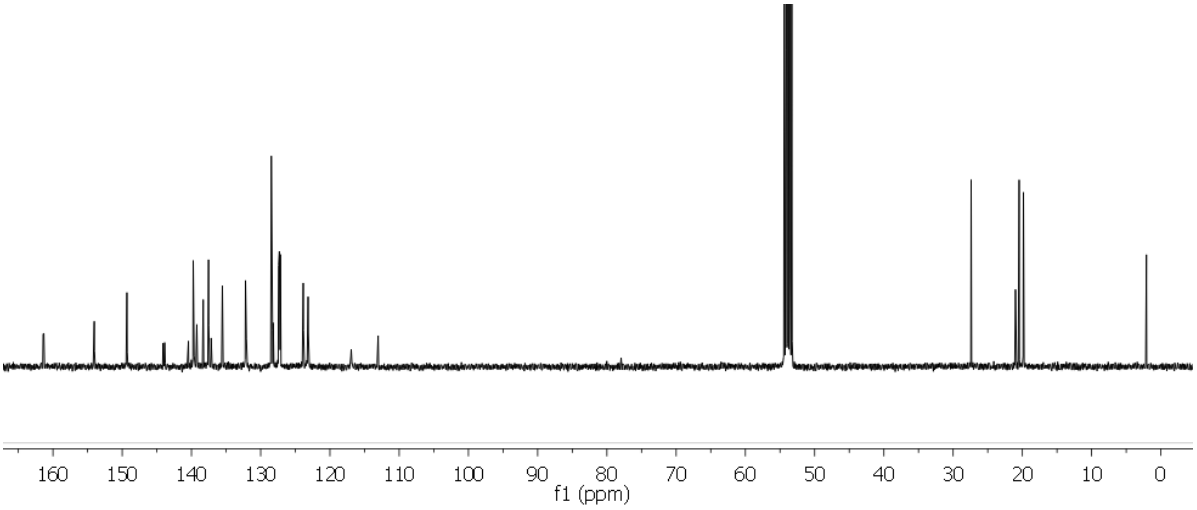

Figure S4. ^{13}C NMR spectrum of [Cu(*trans*-**3**)(**4**)]PF_6 (100 MHz, CD_2Cl_2, 298 K).

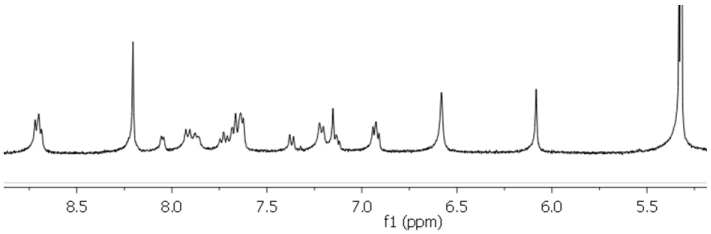

Figure S5. Partial ^{1}H NMR spectrum of [Cu(*trans*-**3**)(**4**)]PF_6 after irradiation for 2 h at 315 nm (400 MHz, CD_2Cl_2, 298 K).

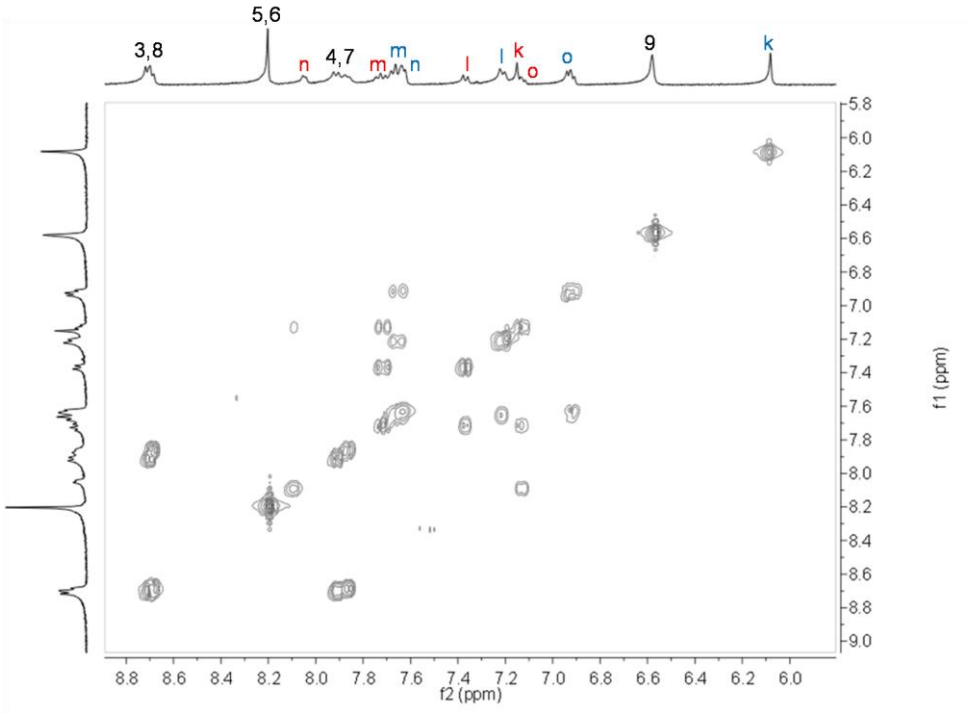

Figure S6. ^{1}H-^{1}H COSY spectrum of [Cu(*trans*-**3**)(**4**)]PF_6 after irradiation for 2 h at 315 nm (400 MHz, CD_2Cl_2, 298 K). Protons for *trans*-**3** are shown in red and for *cis*-**3** in blue.

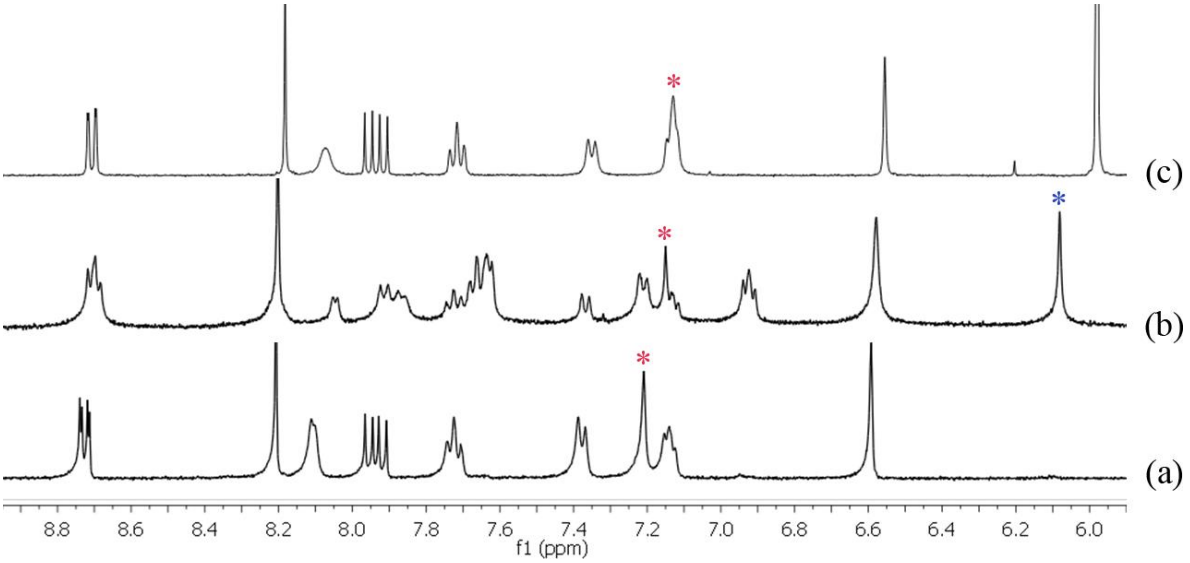

Figure S7. Partial ^{1}H spectra (400 MHz, 298 K) of (a) complex [Cu(*trans*-**3**)(**4**)]PF_6 in CD_2Cl_2, (b) sample (a) after irradiation for 2 h at 315 nm (*trans*:*cis* = 30:70) in CD_2Cl_2 and (c) sample (b) after heating for 24 h at 100 °C in CD_2Cl_4, 100% conversion of *cis*-**3** to *trans*-**3**. (* for *trans* k-H and * for *cis* k-H).

Calculation of *cis*/*trans* ratio

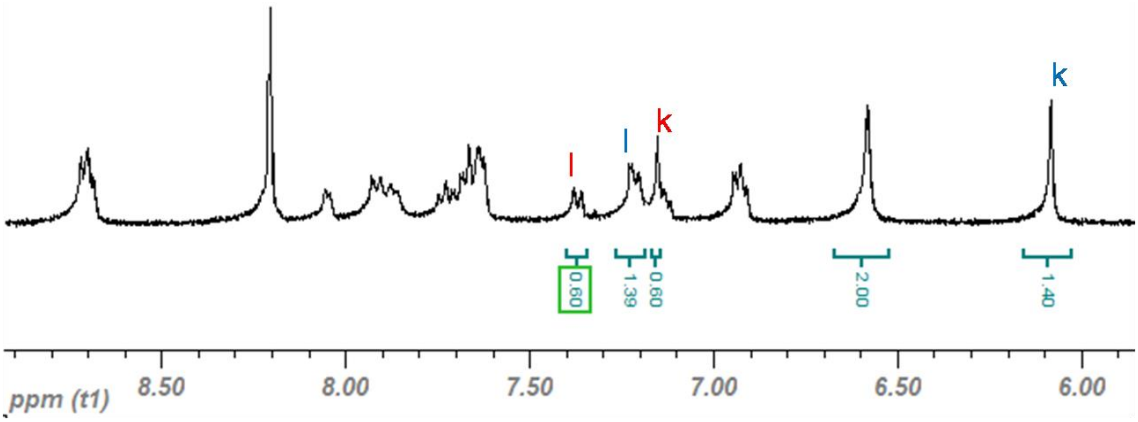

Partial ^{1}H spectrum of [Cu(*trans*-**3**)(**4**)]PF_6 after irradiation at 315 nm for 2 h. Protons for *trans*-**3** are marked in red and for *cis*-**3** in blue.

% of *cis*-**3** (for k-H) = [k-*cis*/(k-*cis* + k-*trans*)] × 100 = [1.40/(1.40 + 0.6)] × 100 = 70%

% of *cis*-**3** (for l-H) = [l-*cis*/(l-*cis* + l-*trans*)] × 100 = [1.39/(1.39 + 0.6)] × 100 = 69.8%

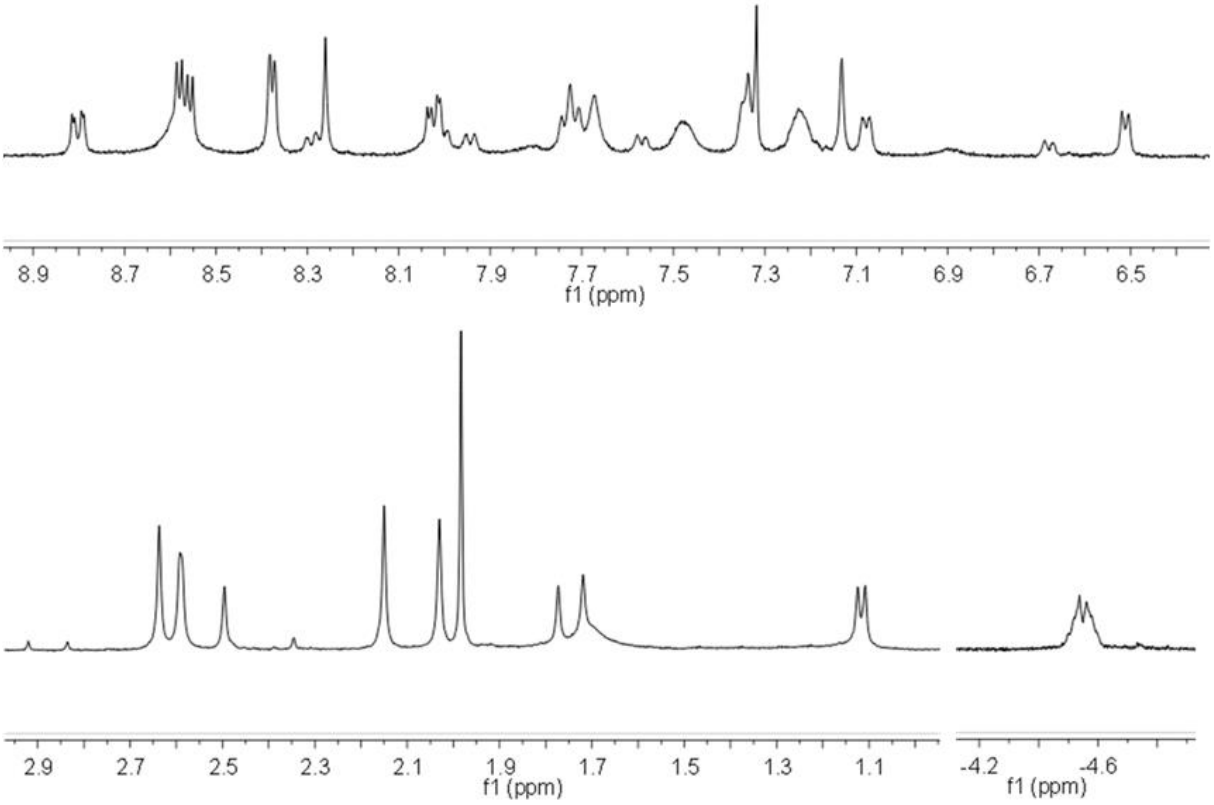

Figure S8. ^{1}H NMR spectrum of **ROT-1** in presence of 2.85 equiv. of *trans*-**3** ($CDCl_3$:CD_2Cl_2 = 1:9, 400 MHz, 298 K).

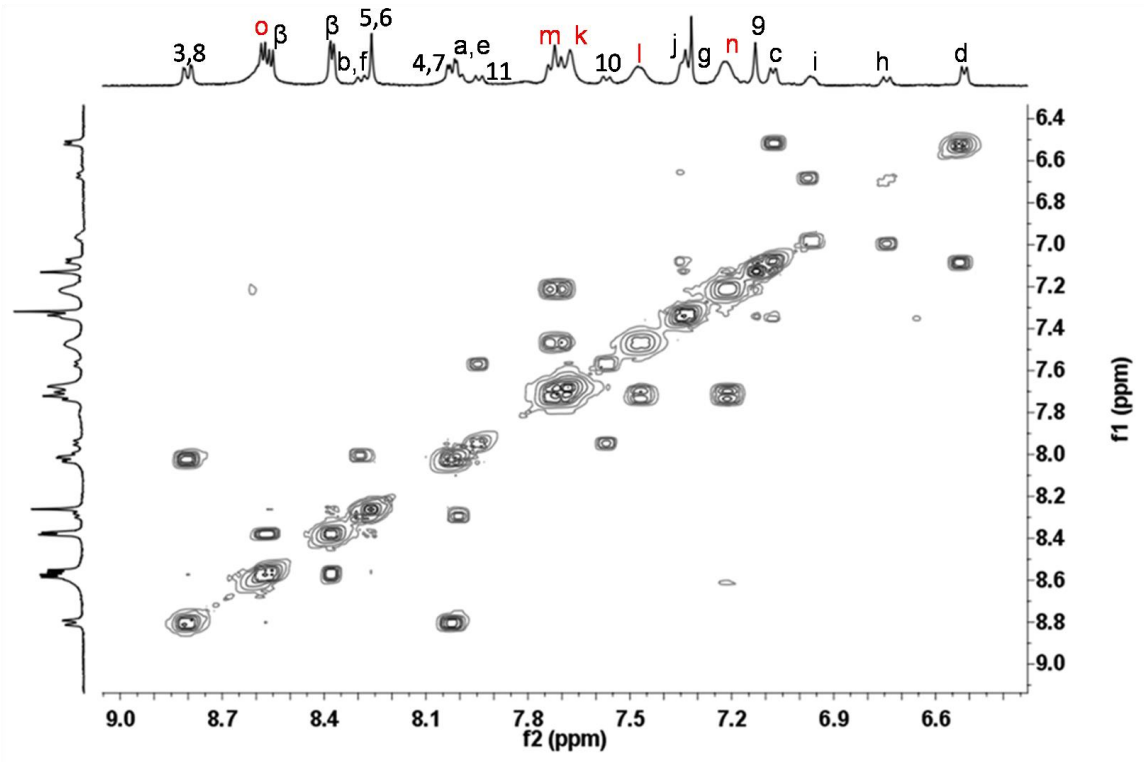

Figure S9. ^{1}H-^{1}H COSY of **ROT-1** in presence of 2.85 equiv. of *trans*-**3** ($CDCl_3$:CD_2Cl_2 = 1:9, 400 MHz, 298 K). Protons for *trans*-**3** are shown in red.

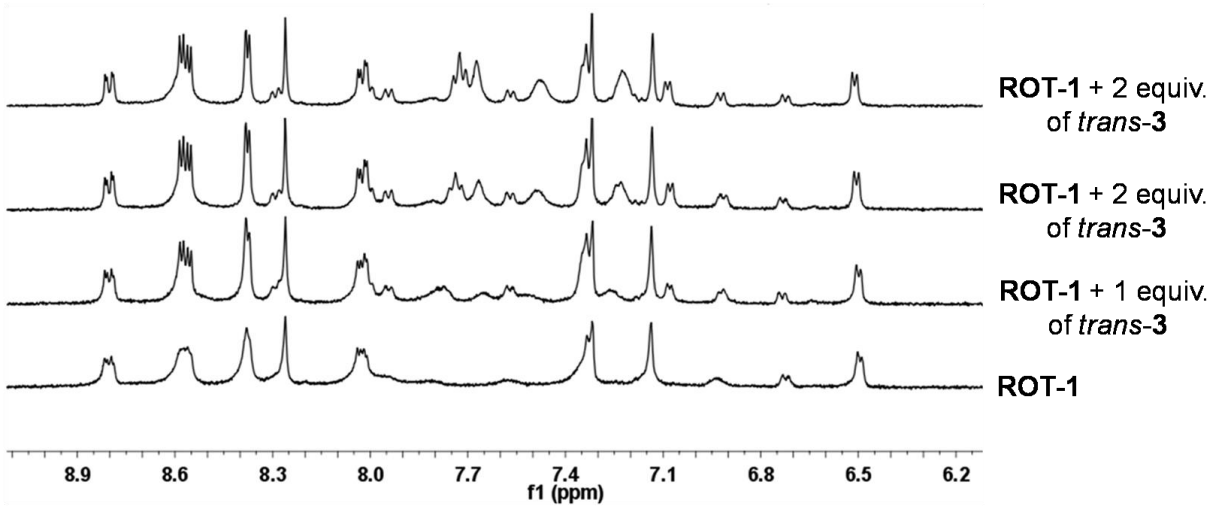

Figure S10. ^{1}H NMR titration of **ROT-1** with *trans*-**3** (**$CDCl_3$:CD_2Cl_2** = 1:9, 400 MHz, 298 K).

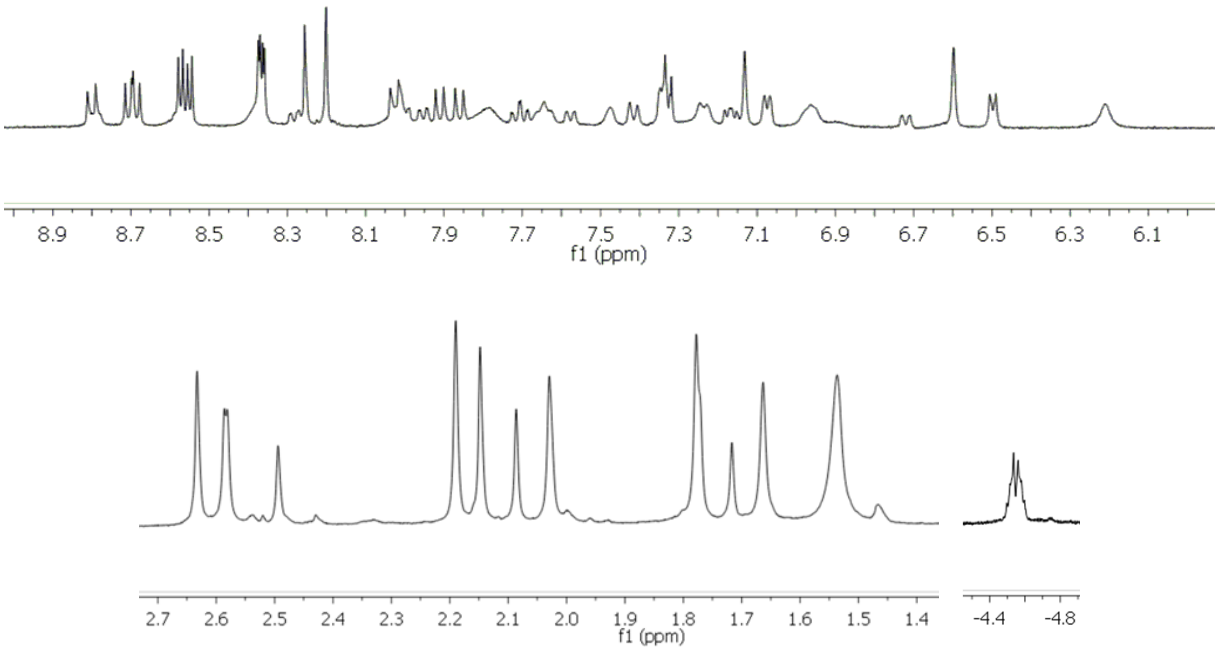

Figure S11. ^{1}H NMR of the mixture of **ROT-1** and 2.85 equiv. of *trans*-**3** after irradiation for 2 h at 315 nm in CD_2Cl_2 (400 MHz, 298 K).

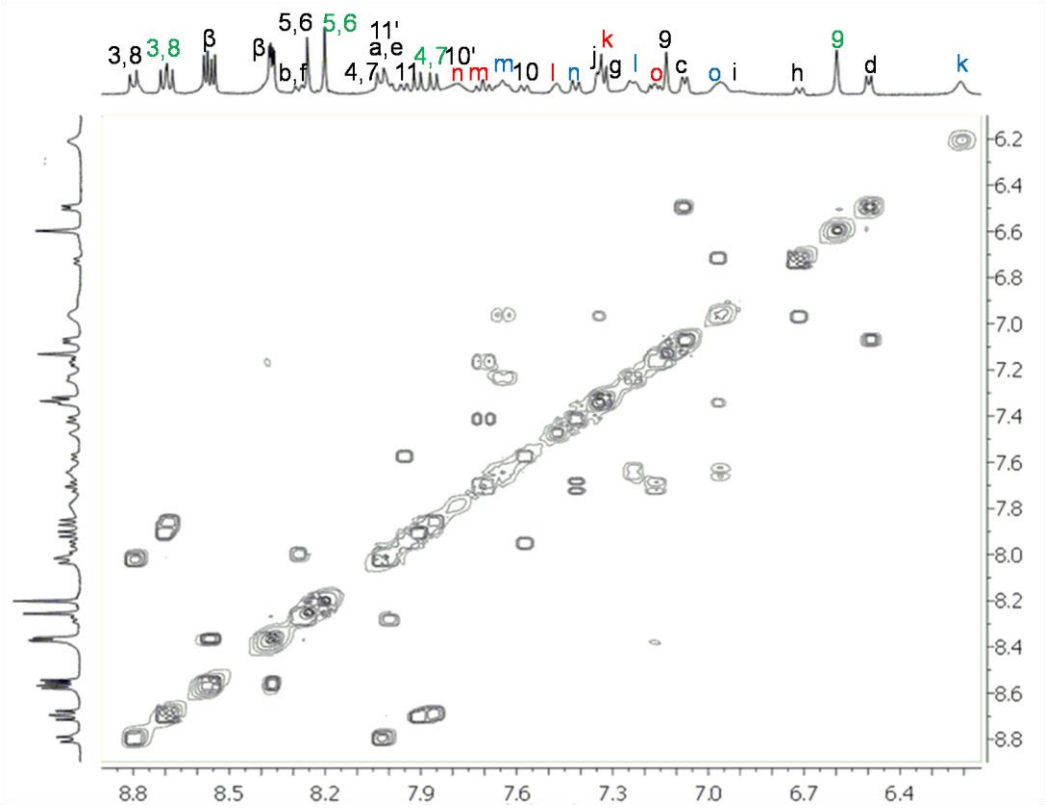

Figure S12. ^{1}H-^{1}H COSY of an irradiated mixture of **ROT-1** and of 2.85 equiv. of *trans*-**3** (400 MHz, CD_2Cl_2, 298 K). Protons for *trans*-**3** are shown in red and *cis*-**3** are in blue. Protons for phenanthrolines involved with *cis*-**3** are shown in green.

Table S1. Resonances of aromatic protons of complex [Cu(*trans*-**3**)(**4**)](PF_6).

Proton assignment	δ / ppm of *trans*-**3**	δ / ppm of phenanthroline
k-H	7.22	
o-H	7.16	
n-H	8.10	
m-H	7.74	
l-H	7.40	
3-H		8.73
4-H		7.96
5-, 6-H		8.21
7-H		7.92
8-H		8.72
9-H		6.60

Table S2. Resonances of aromatic protons of complex [Cu(*trans*-**3**)(**4**)](PF_6) after irradiation.

Proton assignment	δ / ppm of *trans*-**3**	δ / ppm of phenanthroline	δ / ppm of *cis*-**3**
k-H	7.19		6.08
o-H	7.13		6.93
n-H	8.05		7.63
m-H	7.73		7.67
l-H	7.37		7.21
3-H		8.72	
4-H		7.92	
5-, 6-H		8.21	
7-H		7.87	
8-H		8.70	
9-H		6.58	

Table S3. ^{1}H NMR shifts of the aromatic protons of complex **ROT-1** and 2.85 equiv. of *trans*-**3** in a mixture.

δ / ppm of **ROT-1** protons	Proton assignment	δ / ppm of *trans*-**3** protons[a]
8.00	a- and e-H	
8.27	b- and f-H	
7.06	c-H	
6.51	d-H	
7.29	g-H	
6.71	h-H	
6.92	i-H	
7.31,7.33	j-H	
	k-H	7.67
	l-H	7.48
	m-H	7.73
	n-H	7.22

	o-H	8.58
8.03	4-, 7-H	
8.26	5-, 6-H	
8.80	3-, 8-H	
7.10	9-H	
7.58	10- or 11-H	
7.95	11- or 10-H	
8.36, 8.38, 8.56, 8.57	ß-H	

[a] NMR shifts for *trans*-**3** in the mixture are basically identical with those of free *trans*-**3** indicating that *trans*-**3** remains without coordination in the mixture (see Table S4).

Table S4. ^{1}H NMR shifts of the aromatic protons of *trans*-**3**.

Proton assignment	δ / ppm of *trans*-**3** protons[a]	Proton assignment	δ / ppm of *trans*-**3** protons[a]
k-H	7.68	n-H	7.19
l-H	7.44	o-H	8.63
m-H	7.70		

Table S5. ^{1}H NMR shifts of the aromatic protons of [(**ROT-1**)(*cis*-**3**)$_2$] and *trans*-**3** at PSS.

ROT-2 = [(**ROT-1**)(*cis*-**3**)$_2$]				Proton assignment	*trans*-**3**
δ / ppm of *cis*-**3**	δ / ppm of phenanthroline in HETPYP with rotator **2**	δ / ppm of phenanthroline complex with *cis*-**3**	δ / ppm of protons appearing in a single set		
			7.99	a and e-H	
			8.29	b and f-H	
			7.06	c-H	
			6.50	d-H	
			7.31	g-H	
			6.69	h-H	
			6.94	i-H	
			7.34, 7.35	j-H	
6.21				k-H	7.32
7.24				l-H	7.48
7.64				m-H	7.71
7.42				n-H	7.78
6.97				o-H	7.17
	8.80	8.70		3-H	
	8.03	7.91		4-H	
	8.26	8.20		5-, 6-H	
	8.03	7.86		7-H	
	8.80	8.69		8-H	
	7.10	6.60		9-H	
			7.57, 7.95	10- or 11-H	
			7.79, 8.01	10'- or 11'-H	
			8.36, 8.37, 8.56, 8.57	ß-H	

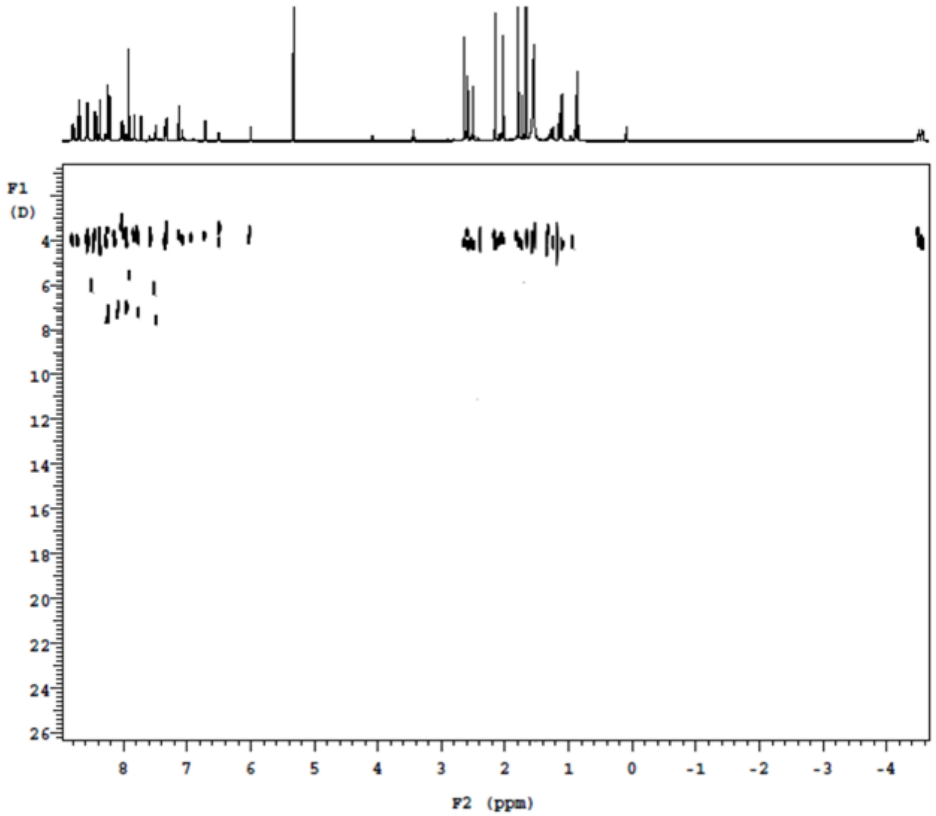

Figure S13. ^{1}H DOSY spectrum of mixture of **ROT-2** and 0.85 equiv. of *trans*-**3** in PSS (CD_2Cl_2, 400 MHz, 298 K).

3. ESI-MS

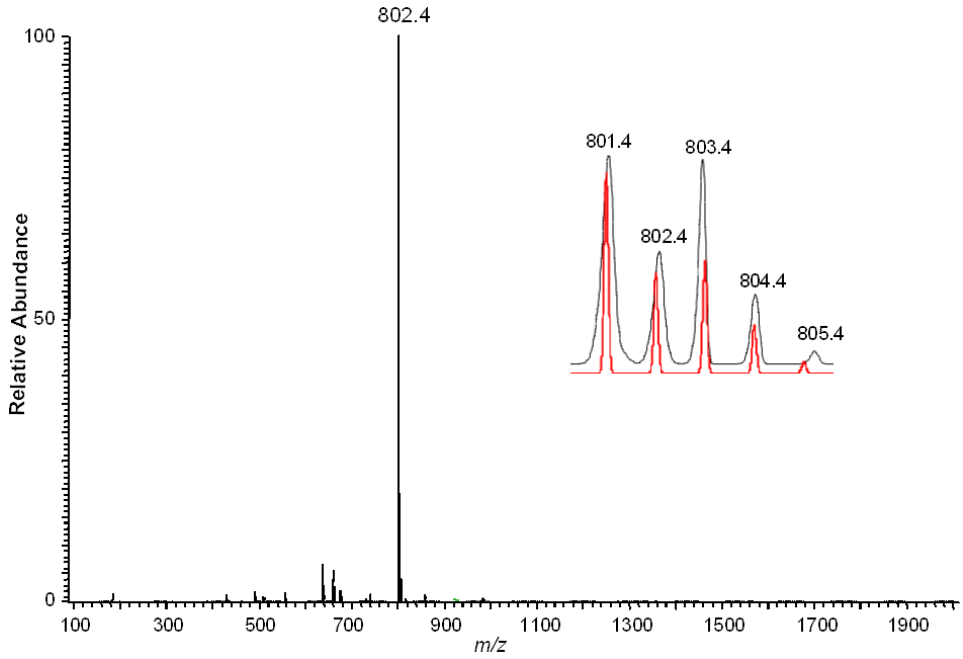

Figure S14. ESI mass spectrum of [Cu(*cis*-**3**)(**4**)](PF$_6$) in CH_2Cl_2.

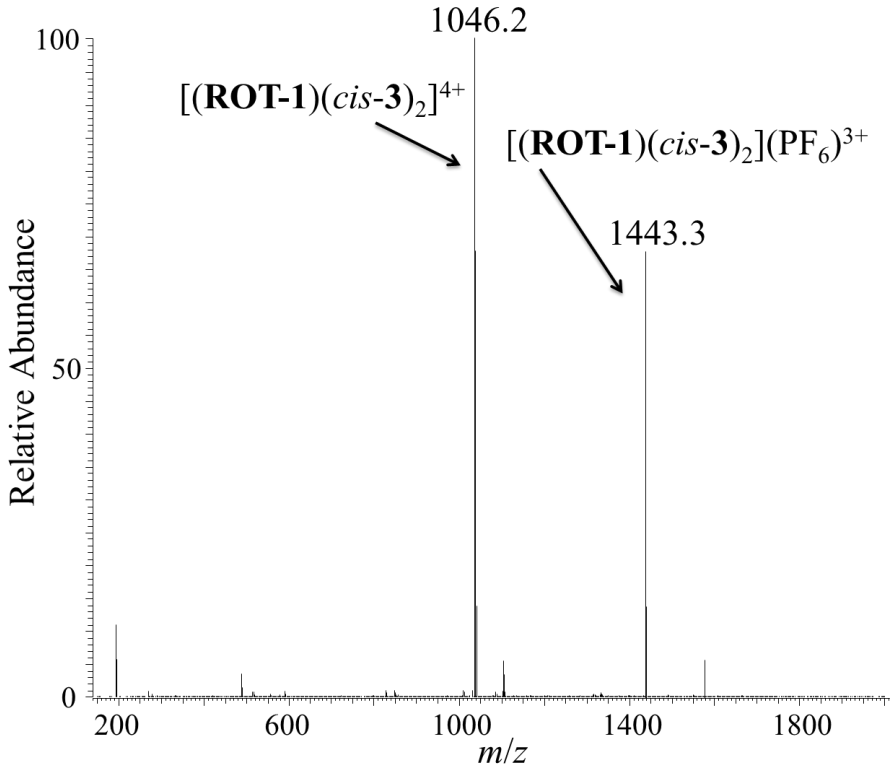

Figure S15. ESI mass spectrum of **ROT-2** in CH_2Cl_2.

4. NMR Lineshape Analysis to Determine the Rates of Spinning

For the spectral simulations[1] we used a conventional dynamic-NMR spectroscopic method based on the model involving a two-spin system undergoing mutual exchange. The protons relevant for the lineshape analysis are indicated in the corresponding spectra by *. Since the rapid spinning motion of the main rotator leads to a degeneracy of the phenanthroline stations, which is best visible at proton 9-H of the stator, the rotational frequency was obtained from an analysis of its exchange-broadened NMR lineshape. Activation enthalpy ($\Delta H^{\ddagger}$) and activation entropy ($\Delta S^{\ddagger}$) were determined from transition state theory. The free activation energy was determined from $\Delta G^{\ddagger}_{298} = \Delta H^{\ddagger} - T\Delta S^{\ddagger}$

The temperature dependence of all rotors was fitted to the Eyring equation[2]:

$k = (k_B T/h)e^{-\Delta G^{\ddagger}/RT}$

$\ln (k/T) = -\Delta H^{\ddagger}/RT + \ln(k_B/h) + \Delta S^{\ddagger}/R$, with R being the universal gas constant.

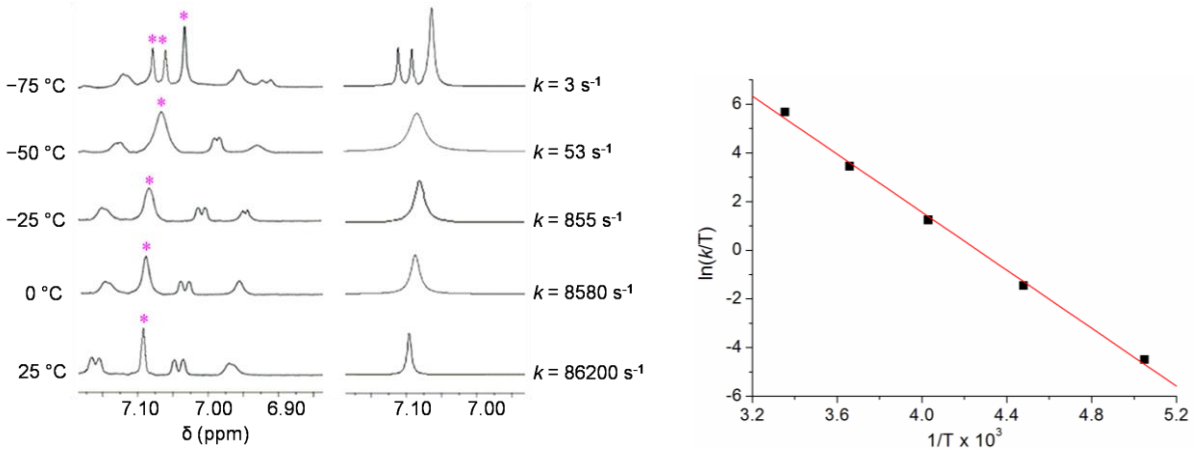

$\Delta H^{‡} = 49.6$ kJ mol^{-1}, $\Delta S^{‡} = 22.0$ J mol^{-1}K^{-1}, $\Delta G^{‡}_{25} = 43.0$ kJ mol^{-1}

Figure S16. (Left) ^{1}H NMR (600 MHz) spectra of a mixture of **ROT-1** and 2.85 equiv. of *trans*-**3** (CD_2Cl_2) at various temperatures (left, experimental and right, simulated) and (Right) Eyring plot for the oscillating rotation in **ROT-1** in presence of 2.85 equiv. of *trans*-**3**.

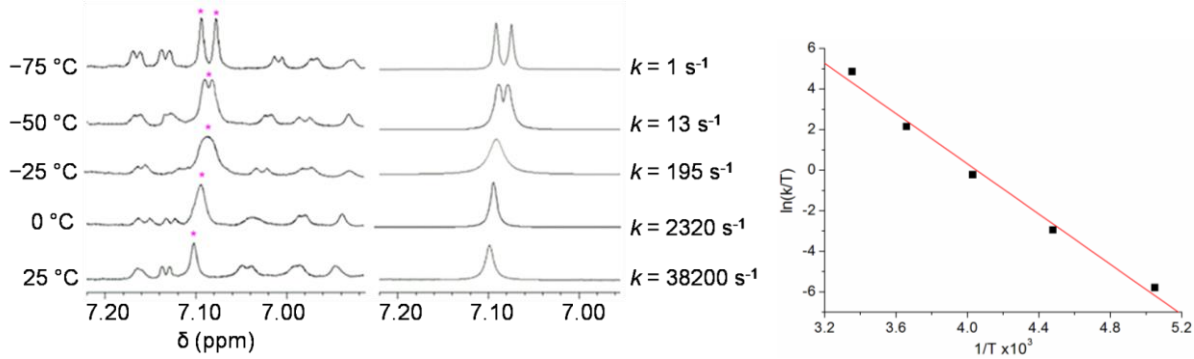

$\Delta H^{‡} = 51.5$ kJ mol^{-1}, $\Delta S^{‡} = 15.0$ J mol^{-1}K^{-1}, $\Delta G^{‡}_{25} = 47.0$ kJ mol^{-1}

Figure S17. Eyring plot for the oscillating rotation in **ROT-2** = [(**ROT-1**)(*cis*-**3**)$_2$].

5. UV-Vis Investigations

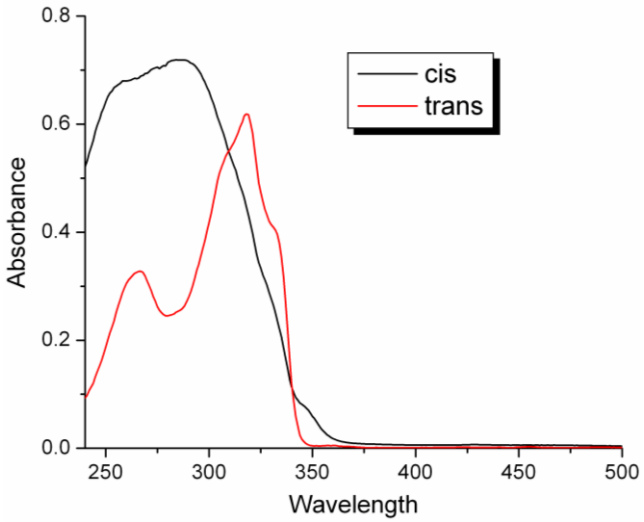

Figure S18. UV-Vis spectra of **3** in CH_2Cl_2 at 25 °C.

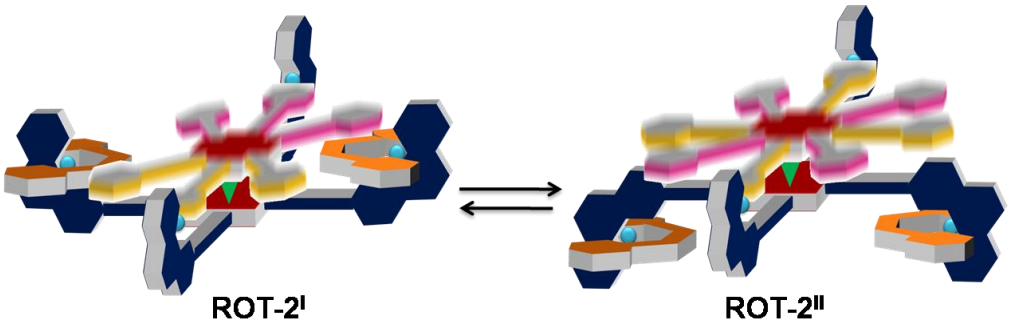

Figure S19. Two selected conformations of the 5-component nanorotor **ROT-2**. Conformation **ROT-2^{I}**: The side rotators are within the trajectory of the main rotator thus interfering with the rotation. Conformation **ROT-2^{II}**: Both side rotators are outside of the trajectory of the main rotator allowing uninhibited motion.

6. X-ray Crystal Structure Analysis of $[Cu_2(\textit{trans}\text{-}3)(4)_2](PF_6)_2$

X-ray single-crystal diffraction data was collected on a SIEMENS SMART 1K CCD diffractometer with Mo Kα radiation. The structure was determined using program SHELXS-97 and refined by full-matrix least-squares using program SHELXL-97.[3] The hydrogen atoms were generated theoretically onto the specific atoms and were treated as riding atoms. The non-hydrogen atoms were refined with anisotropic thermal parameters. Further details are provided in the table below.

The $[Cu_2(\textit{trans}\text{-}\mathbf{3})(\mathbf{4})_2]^{2+}$ is centrosymmetric and has a crystallographic inversion center at the midpoint of the central C=C double bond. It contains two 2-(2,3,5,6-tetramethyl-4-iodophenyl)-9-(2,4,6-trimethylphenyl)[1,10]-phenanthroline (**4**) units and a *trans*-1,2-bis(2-pyridyl)ethylene (*trans*-**3**) group connected by two copper(I) ions. The Cu atom has a heavily distorted trigonal coordination of N atoms. The $Cu\text{-}N_{phenanthroline}$ bond distances are 2.039(4) and 2.076(4) Å and the $Cu\text{-}N_{pyridyl}$ bond distance is 1.932(4) Å.

The phenanthroline group only shows a very small distortion from planarity, the mean deviation from the best plane is 0.028 Å. The angle between the plane of the phenanthroline group and the planes of the 2,4,6-trimethylphenyl (mesityl) and 2,3,5,6-tetramethyl-4-iodophenyl groups is 65.9 and 77.0°, respectively. The angle between the planes of the latter two groups is 55.6°. The pyridyl group is almost coplanar with the 2,3,5,6-tetramethyl-4-iodophenyl group (angle between planes: 3.5°). The crystal packing shows 10 intermolecular C-H…F contacts with H…F distances between 2.39 and 2.65 Å.

Crystal Data for complex $[Cu_2(\textit{trans}\text{-}3)(4)_2](PF_6)_2$:

CCDC	975665	
Empirical formula	$C_{74}H_{68}Cu_2F_{12}I_2N_6P_2$	
Formula weight	1712.16	
Temperature	171(2) K	
Wavelength	0.71073 Å	
Crystal system	Triclinic	
space group	*P* -1 (Nr. 2)	
Unit cell dimensions	a = 11.4761(6) Å	α = 107.8770(10)°
	b = 12.0349(6) Å	β = 106.8250(10)°

	c = 14.8885(7) Å γ = 101.5750(10)°
Volume	1776.14(15) $Å^3$
Z	1
Density (calculated)	1.601 $g.cm^{-3}$
Absorption coefficient	1.592 mm^{-1}
F(000)	856
Crystal size	0.40 x 0.40 x 0.30 mm^3
Theta range for data collection	1.6 to 26.2°.
Limiting indices	$-14\leq h\leq 14$, $-14\leq k\leq 14$, $-18\leq l\leq 18$
Reflections collected / unique	18413 / 6778 [R_{int} = 0.049]
Completeness to theta = 25.0°	98.8 %
Absorption correction	Semi-empirical from equivalents
Max. and min. transmission	0.620 and 0.446
Refinement method	Full-matrix least-squares on F^2
Data / restraints / parameters	6778 / 0 / 449
Goodness-of-fit on F^2	1.08
Final R indices [I>2σ(I)]	R1 = 0.061, wR2 = 0.158
R indices (all data)	R1 = 0.085, wR2 = 0.171
Largest diff. peak and hole	2.11 and –1.32 $e.Å^{-3}$

Selected bond lengths (Å) and bond angles (°).

Cu(1)_N(1)	2.076(4)
Cu(1)-N(2)	2.039(4)
Cu(1)-N(3)	1.932(4)
N(1)-Cu(1)-N(2)	80.86(15)
N(1)-Cu(1)-N(3)	130.68(16)
N(2)-Cu(1)-N(3)	145.92(16)

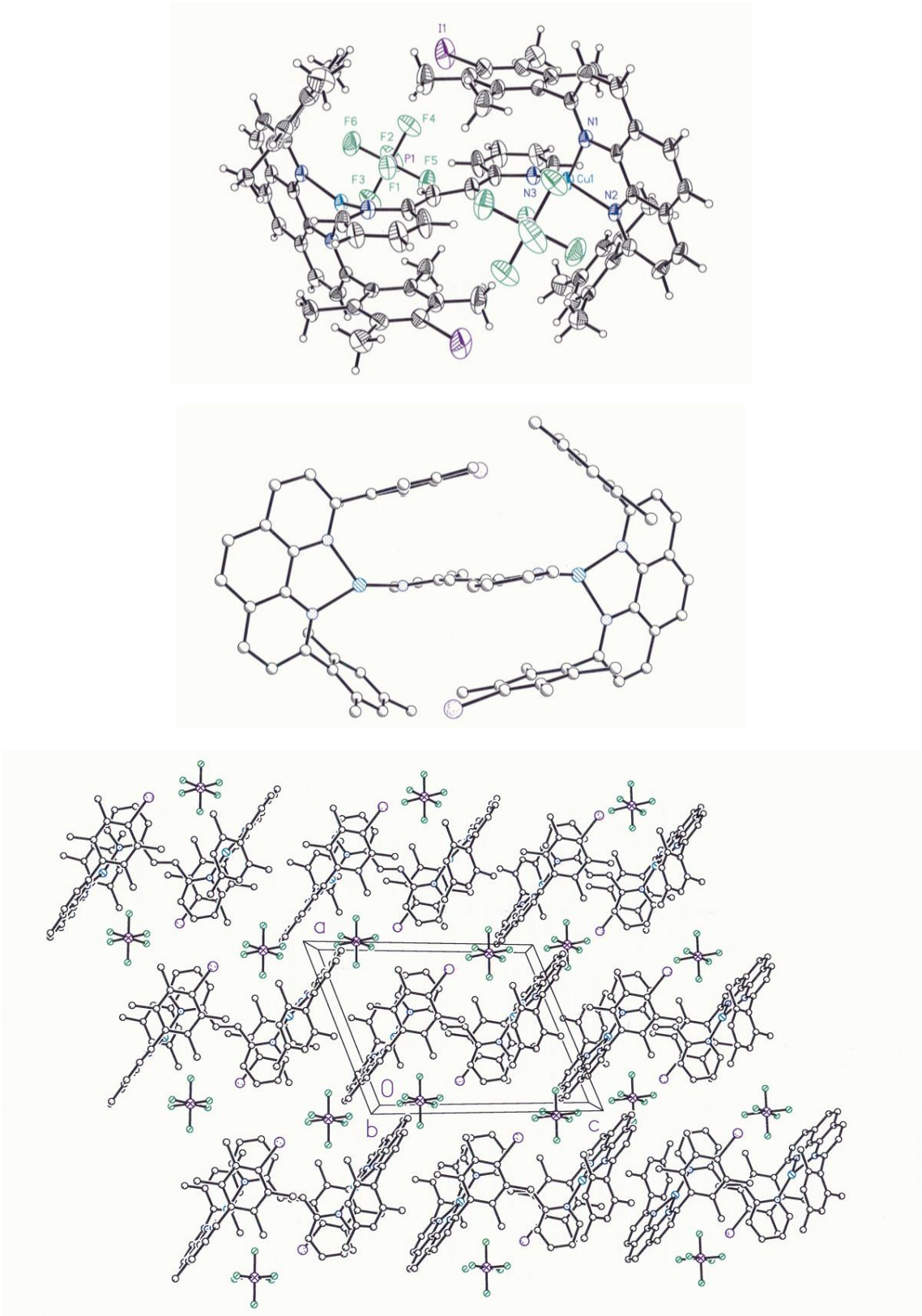

Figure S20. (Top) Crystal structure of complex $[Cu_2(\textit{trans}\text{-}\mathbf{3})(\mathbf{4})_2](PF_6)_2$. Thermal ellipsoids are drawn at the 50% probability level. (Middle) View of the cation showing the relative orientations of the planar groups. (Bottom) Packing diagram along the b-axis. Hydrogen atoms omitted for clarity.

7. Computed Structure of [Cu(*cis*-3)(4)]$^+$

The energy-minimised structure of [Cu(*cis*-**3**)(**4**)]$^+$ was calculated using Gaussian03 at the B3LYP/6-31G* level, applying the LANL2DZ[4] effective core potential for copper.

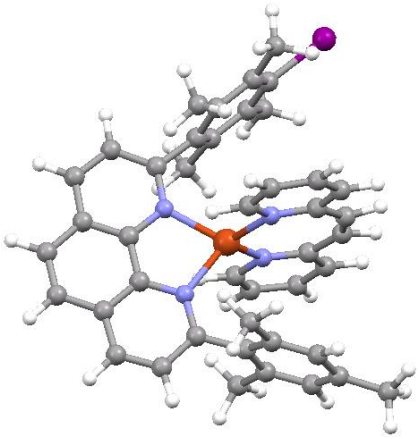

Figure S21. Optimised structure of [Cu(*cis*-**3**)(**4**)]$^+$.

Table S6. X,Y,Z cartesian coordinates of complex [Cu(*cis*-**3**)(**4**)]$^+$.

C	-4.199600	0.910900	0.000000	H	5.850100	-3.790800	-0.888000
C	-5.021600	-0.196300	0.000000	H	5.850100	-3.790800	0.888000
C	-4.454400	-1.493100	0.000000	C	-2.025300	1.950700	2.545700
C	-3.041800	-1.576200	0.000000	H	-2.662900	2.675300	3.065200
C	-2.793200	0.753400	0.000000	H	-2.621500	1.048400	2.398100
C	-5.231200	-2.698700	0.000000	H	-1.209400	1.695200	3.229000
C	-2.404200	-2.862000	0.000000	C	-0.295500	4.329300	2.544100
C	-3.195100	-4.034900	0.000000	H	-0.695000	3.810700	3.414400
C	-4.624900	-3.921200	0.000000	H	0.794600	4.367800	2.647700
C	-2.508200	-5.272100	0.000000	H	-0.650900	5.364600	2.585600
H	-3.073100	-6.200300	0.000000	I	0.960800	5.935600	0.000000
C	-1.129900	-5.288500	0.000000	C	-2.025300	1.950700	-2.545700
C	-0.397100	-4.076500	0.000000	H	-2.621500	1.048400	-2.398100
H	-6.314100	-2.619500	0.000000	H	-2.662900	2.675300	-3.065200
H	-4.610500	1.915000	0.000000	H	-1.209400	1.695200	-3.229000
H	-6.102100	-0.082500	0.000000	C	-0.295500	4.329300	-2.544100
H	-5.218100	-4.830700	0.000000	H	0.794600	4.367800	-2.647700
H	-0.581200	-6.224200	0.000000	H	-0.695000	3.810700	-3.414400
N	-2.245300	-0.465600	0.000000	H	-0.650900	5.364600	-2.585600
N	-1.038700	-2.900700	0.000000	Cu	-0.249900	-0.993300	0.000000
C	-1.882400	1.946700	0.000000	C	0.172100	-0.824900	2.836000
C	-1.510200	2.521200	1.238400	C	2.075700	0.041500	1.810600
C	-1.510200	2.521200	-1.238400	C	0.675900	-0.630600	4.116500
C	-0.698600	3.672200	1.244200	H	-0.815200	-1.255800	2.701500
C	-0.698600	3.672200	-1.244200	C	2.639300	0.264700	3.085200
C	-0.297500	4.202100	0.000000	C	1.947100	-0.070500	4.241400
C	1.098600	-4.084500	0.000000	H	0.086300	-0.911900	4.982400
C	1.796800	-4.133900	-1.229100	H	3.628900	0.702700	3.155200
C	1.796800	-4.133900	1.229100	H	2.389400	0.102200	5.217800

C	3.192900	-4.166200	-1.201400	C	0.172100	-0.824900	-2.836000
C	3.192900	-4.166200	1.201400	C	2.075700	0.041500	-1.810600
C	3.913300	-4.180400	0.000000	C	0.675900	-0.630600	-4.116500
H	3.734600	-4.205900	-2.143700	H	-0.815200	-1.255800	-2.701500
H	3.734600	-4.205900	2.143700	C	2.639300	0.264700	-3.085200
C	1.078400	-4.245000	2.556100	C	1.947100	-0.070500	-4.241400
H	0.152100	-3.664500	2.591800	H	0.086300	-0.911900	-4.982400
H	0.810800	-5.289200	2.765200	H	3.628900	0.702700	-3.155200
H	1.718700	-3.910200	3.376900	H	2.389400	0.102200	-5.217800
C	1.078400	-4.245000	-2.556100	N	0.836200	-0.507500	-1.705800
H	0.810800	-5.289200	-2.765200	N	0.836200	-0.507500	1.705800
H	0.152100	-3.664500	-2.591800	C	2.915300	0.443500	0.679500
H	1.718700	-3.910200	-3.376900	C	2.915300	0.443500	-0.679500
C	5.419100	-4.263100	0.000000	H	3.836900	0.874200	1.063200
H	5.746900	-5.311000	0.000000	H	3.836900	0.874200	-1.063200

(1) H. J. Reich, *NMR Spectrum Calculations: WinDNMR, Version 7.1.13.* Department of Chemistry, University of Wisconsin.

(2) H. L. Eyring, *J. Chem. Phys.* 1935, **3**, 107.

(3) (a) G. M. Sheldrick, *SHELXS97: Program for Crystal Structure Determination*; University of Göttingen: Göttingen, Germany, 1997. (b) G. M. Sheldrick, *SHELXL97*: *Program for Crystal Structural Refinement*; University of Göttingen: Göttingen, Germany, 1997.

(4) P. J. Hay and W. R. Wadt, *J. Chem. Phys.* 1985, **82**, 299.